# Active Cancelling System for Mitigating ELFM Field in a High Tech Fab



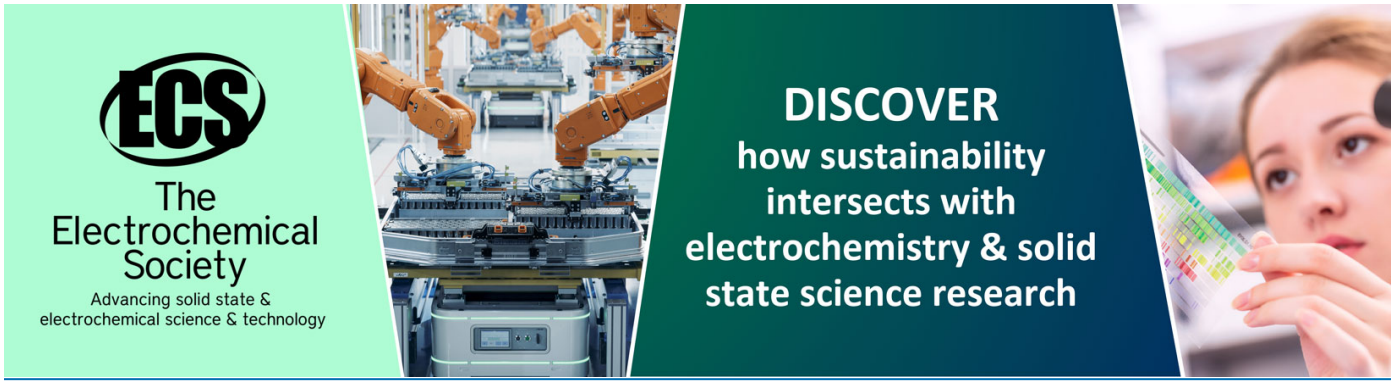

# Active Cancelling System for Mitigating ELFM Field in a High Tech Fab

**H Y Lin and L M Chang**

High-Tech Facility Research Center, National Taiwan University Zhubei Campus
No.88 Zhuangjing 1st Rd., Hsinchu, 30264 Taiwan

hungyilin@ntu.edu.tw

**Abstract.** As nano-level of semiconductor manufacturing technology continuously advances, the demands of the high performance microscopes (HPM) and other precision instruments are increasing. To employ these microscopes and instruments, the processes involved are often venerable to electromagnetic interference (EMI), especially, the processes would be sensitively impacted by the extremely low frequency magnetic (ELFM) field. The frequency ranges of the ELFM field are from 1Hz to 3KHz. The high-intensity of ELFM field would cause measurement errors of high-precision instruments and drop production yield rate. In this paper, an active magnetic interference cancelling system (AMICS) with square Helmholtz coil structure will be utilized. The square Helmholtz coil structure is used for generating a magnetic field for mitigating the ELFM. To achieve the fast response of AMICS in regard to the ELFM field change, an embedded system with the real-time operating system (RTOS) was built to perform the magnetic measurement and magnetic cancelling task. The experimental results of research show that the ELF field cancelling capability has been improved about 95.87% for 60Hz and 96.05% for 100Hz.

## 1. Introduction

In order to measure and to make nanostructure, many delicate and precise high performance tools are used for high-tech semiconductor fabrication. The images of the high precision measurement instruments such as scanning electron microscope (SEM), transmission electron microscope (TEM), focused ion beam (FIB) and electron beam lithography are often spoilt by the environmental magnetic interference from the movement of automated material handling system (AMHS) or other high power production equipment [1]. A magnetic shielding room (MSR) with material of high permeability is used for reducing such interference. Nevertheless, there are two disadvantages. The first one is that the cost of this shielding method is expensive. The second one is that the shielding factor in the low frequency range is small.

In reviewing related literature, a variety of AMICS schemes has been developed to improve the shielding effect in the low frequency range. A low temperature superconducting quantum interference device ($LT_c$-SQUID) sensor with proportional integral differential (PID) controller is equipped for biomagnetic measurement. By using the $LT_c$-SQUID sensor, the sensitivity of the measurement system for the frequency range from 10mHz to 100Hz can be enhanced [2]. To design the efficient shields, a new shield's shape optimization technique for low frequency magnetic field has been simulated by using the genetic algorithm (GA) and finite element method (FEM) [3]. A symmetric magnetic field sensor method is utilized to solve the problems of the magnetic field sensor position

and cross axial interference [4]. However, the drawback of this method is that six magnetic field sensors are positioned for three-axis magnetic sensing.

The purpose of this paper is to present the experimental findings resulted from developing the real-time AMICS for mitigating environmental ELFM interference. The brief theoretical analysis is introduced in Section 2. The system architecture and hardware design is discussed in Section 3. Software design is discussed in Section 4. Finally, Section 5 shows the experimental setting and results.

## 2. Theoretical basic for square Helmholtz coil

The configuration of the single square Helmholtz coil is shown in figure 1, the mathematical model of the square Helmholtz coil based on the magnetic field expression of the Biot-Savart law is shown in following equation (1).

$$dB = \mu_0 \frac{I}{4\pi} \cdot \frac{d\vec{l} \times \vec{r}}{r^3} \tag{1}$$

Where $\vec{r}$ is the vector from the differential current element at the field point P. $d\vec{l}$ represents the unit length vector of the current element. $\mu_0$ is for vacuum permeability. $I$ indicates the current flowing through the element.

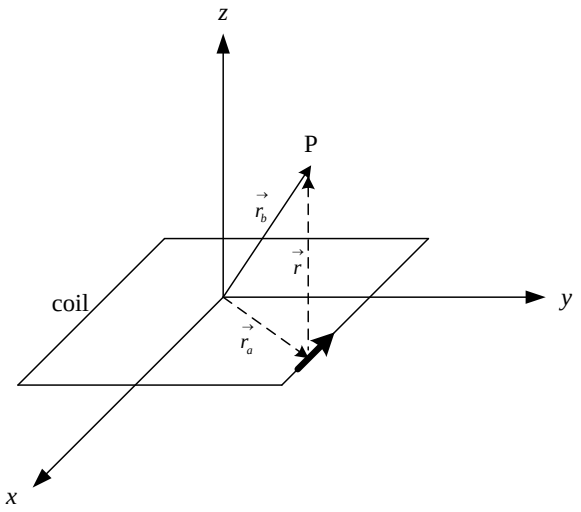


**Figure 1.** The square Helmholtz coil configuration

It is considered that the pair square Helmholtz coils lie on the x-y plane with $L$ distance, and the magnetic field at the point P can be obtained by integrating equation 1. By summing the two magnetic field at point P on z-axis, the equation (2) expresses the total magnetic field [5] [6].

$$B_z(z) = 2\frac{\mu_0}{\pi} IL^2 \cdot \left[ \frac{1}{4z^2 + 4dz + d^2 + L^2 \sqrt{z^2 + dz + \frac{d^2}{4} + \frac{L^2}{2}}} + \frac{1}{4z^2 - 4dz + d^2 + L^2 \sqrt{z^2 - dz + \frac{d^2}{4} + \frac{L^2}{2}}} \right] \tag{2}$$

The simulation results of B field are shown in figure 2 [7]. The simulated setting of the software is that the coil length is 2m, coil spacing is 2m and the current is 3A.

## 3. System architecture of AMICS

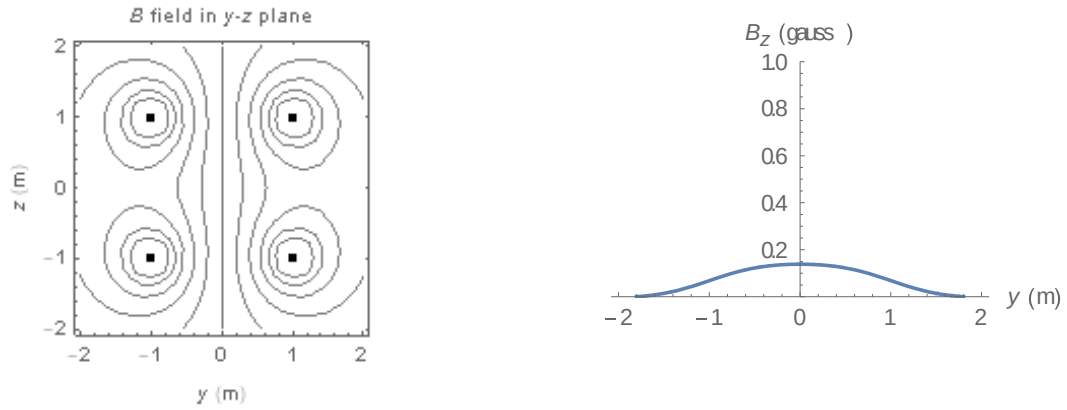


**Figure 2**. The simulation results of B fields of our experimental setting

Figure 3 shows the function block of the AMICS for mitigating the ELFM. There are three sub-blocks within the AMICS which are analog front end (AFE) block, digital processing (DP) block and output control (OC) block. AFE is used for sensing and amplifying the small ELFM signal. HMC2003 (Honeywell) is a three-axis magneto-resistive sensor with high sensitivity. Three precision low-noise instrumentation amplifiers with 1KHz low pass filter provide accurate measurements while rejecting unwanted noise. DP block has a 16-bit high resolution analog to digital converter (ADC) and a STM32F429 32 bits ARM-based embedded system. Analog ELMF electronic signal converted by HMC2003 sensor is transformed into digital signal by ADC, and then it is processed by the embedded system. Unity gain buffer is used for enhancing the driving capability of ADC, so the signal degradation can be prevented.

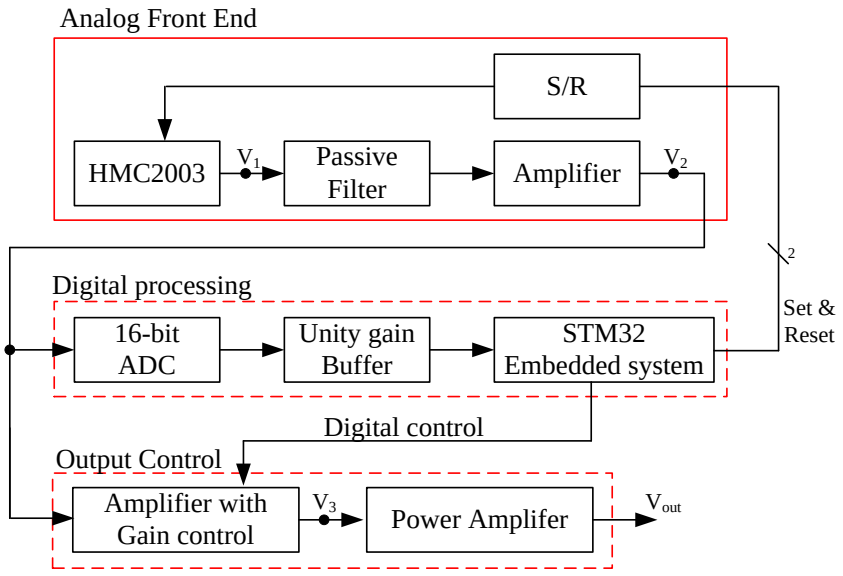


**Figure 3.** The function block of the proposed AMICS system

Amplifier with gain control within the OC is used for controlling the output signal level of AMICS, and the gain is controlled by the embedded system. The output of the embedded system generates digital control code to counter up or counter down, so the gain of the amplifier can be adjusted dynamically. Figure 4 shows the implementation of the passive filter and amplifier in AFE block. $R_1$ and $C_1$ form a passive filter, and the cut-off frequency of the passive filter is $\frac{1}{2\pi R_1 C_1}$. *U1* forms a unity gain buffer which is used for frequency compensation. *U2, $R_2$, $R_3$, $R_4$* and $R_5$ form an inverter amplifier. HMC2003 sensor is implemented in four-element form known as a wheatstone bridge. The bridge sensor offers many desirable characteristics, but one undesirable characteristic is an output voltage without any detected sensor stimulus known as an offset voltage. This offset voltage may cause reduced performance.

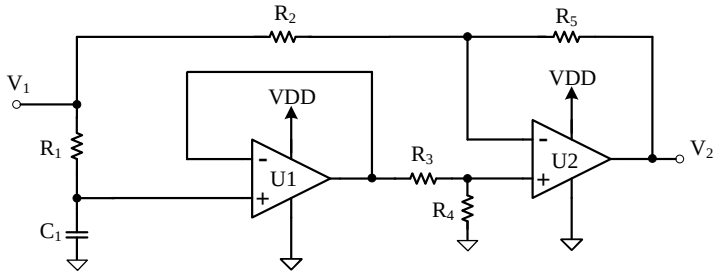


**Figure 4.** The implementation of the passive filter and amplifier in the AFE block

of the sensor system if not compensated for [8]. Figure 5 shows the offset compensation circuit which is S/R circuit in AFE block. When set pulse is high and transistor *Q1* is turned on, the charging current, $I_{ch}$, is flow from *VDD_H* to $C_2$. While reset pulse is high, transistor *Q2* is turned on and transistor *Q1* is turned off, the discharging current, $I_{disc}$ is flow from $C_2$ to ground. *U3* and *U4* are buffers to improve the driving capability of the set and reset signal respectively. Figure 6 show the schematic of the amplifier with gain control in OC block. Digital potentiometer $VR_1$ is used for adjusting the gain of the amplifier *U5*. The digital steps of the potentiometer $VR_1$ are controlled by embedded system. Comparing with the inverse polarity waveform generated by embedded system, the advantage of this OC architecture is that it can quickly respond to the change of the magnetic field.

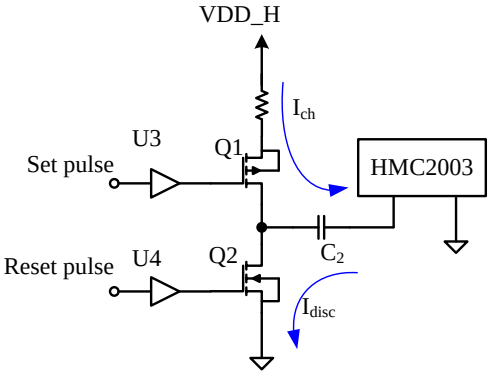


**Figure 5**. The S/R circuit in the AFE block

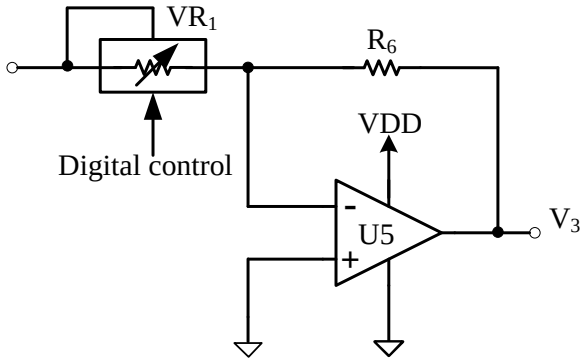


**Figure 6.** The implementation of the amplifier with gain control.

## 4. Software design of AMICS

The software flow diagram of the AMICS is shown in figure 7. The free RTOS is built in STM32F429 embedded system for real-time processing. There are two tasks, one is magnetic measured task, and the other one is magnetic cancelling task. Scheduler is used for arranging the task switching. As mentioned in Section 3, set pulse and reset pulse are performed to cancel the offset of the sensor.

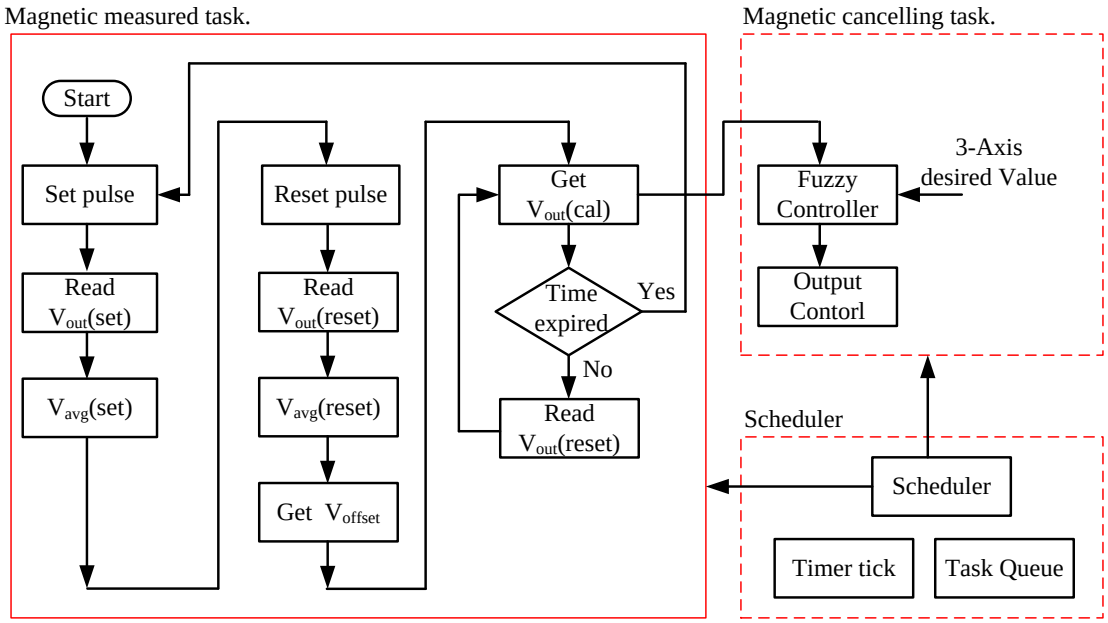


**Figure 7**. The software block of the AMICS

In magnetic measured task, set pulse is stimulated first, and the output of amplifier $V_2$ shown in figure 5 is input to the 16-bit ADC. To remove the device noise or device bias, the accumulation and average of the *Vout(set)* shown in equation (3) and *Vout(reset)* shown in equation (4) are performed respectively.

$$V_{avg}(set) = \frac{\sum_{N=0}^{19} V_{out}(set_{\_N})}{20} \tag{3}$$

$$V_{avg}(reset) = \frac{\sum_{N=0}^{19} V_{out}(reset_{\_N})}{20} \tag{4}$$

The offset voltage of the HMC2003 is obtained by equation (5). By using the $V_{offset}$, the measured output $V_{out}(cal)$ is given by equation (6)

$$V_{offset} = \frac{V_{avg}(set) + V_{avg}(reset)}{2} \tag{5}$$

$$V_{out}(cal) = V_{avg}(reset) - V_{offset} \tag{6}$$

In magnetic cancelling task, the fuzzy controller is designed to adjust the difference between $V_{out}(cal)$ and the desired 3-axis value adaptively. The scheduler is used for switching two different tasks by trigging the timer tick.

## 5. Experimental results

Figure 8 shows how the experimental was set. We use tenmars magnetic field meter as a tool for comparing the mitigating ELFM field result of our AMICS. The experimental result is listed in table 1. Comparing the mitigate interference before and after cancellation, the experimental results showed that the improvement of the shielding capability for 60Hz is 95.87%, for 100Hz is 96.05% and for 150Hz is 93.52%.

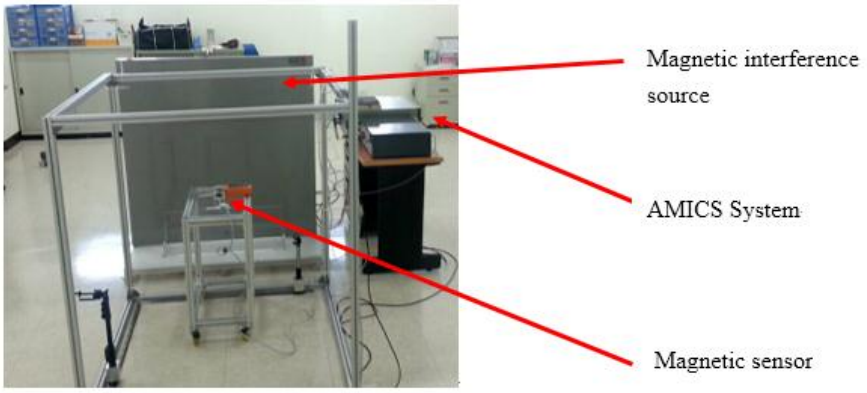


**Figure 8.** The experiment setup of the AMICS

**Table. 1** The experimental results of AMICS before and after cancellation.

| Frequency | 60Hz | | 100Hz | | 150Hz | |
|---|---|---|---|---|---|---|
| Cancelling | Before | After | Before | After | Before | After |
| Max (mGauss) | 14.7 | 0.7 | 14.7 | 0.6 | 13.8 | 1 |
| Min (mGauss) | 14.3 | 0.5 | 14.5 | 0.5 | 13.5 | 0.7 |
| Average (mGauss) | 14.517 | 0.6 | 14.53 | 0.573 | 13.687 | 0.887 |
| Variance | 4.20E-03 | 2.07E-03 | 4.24E-03 | 2.02E-03 | 6.02E-03 | 5.33E-03 |
| Std deviation | 6.37E-02 | 4.47E-02 | 6.40E-02 | 4.42E-02 | 7.63E-02 | 7.18E-02 |
| Shield capability | 95.87% | | 96.05% | | 93.52% | |

## 6. Conclusions

This paper presents the experimental AMICS by using the magnetoresistive sensor to measure and mitigate the ELFM field. To achieve proper response to the change of ELFM field, the magnetic measured task and the magnetic cancelling task are scheduled by freeRTOS. Moreover, the fuzzy controller is designed to adjust the difference between measured output of the sensor and the desired 3-axis value adaptively. The experimental results demonstrate that the ELF field cancelling capability has been improved up to 95.87% for 60Hz, 96.05% for 100Hz and 93.52% for 150Hz, respectively.

## Acknowledgements

The authors would like to thank Taiwan Ministry of Science and Technology (MOST) for sponsoring this research under the Grant No. MOST 107-2221-E-027-109-MY2 and Wolfram for providing Mathematica Simulation Software.

## References

[1] Chang L M 2007 High-Tech Facility Engineering in NT Era *CECI engineering technology*, CECI, Taipei, Taiwan, vol.74, p 22-37.

[2] Platzek D, Nowak F, Giessler F, RÖther J and Eiselt 1999 Active Shield to Reduce Low Frequency Disturbances in Direct Current near Biomagnetic Measurements *Review of Scientific Instruments*, AIP, vol. 70(5), p 2465-2470.

[3] Ziolkowski M, and Gratkowski S 2009 Active, Passive and Dynamic Shielding of Static and Low Frequency Magnetic *International Sym. On Theoretical Eng.*, ISTET'09, p 370-374.

[4] Kobayashi K, Kon A, Yoshizawa M, and Uchikawa Y 2012 Active Magnetic Shielding Using Symmetric MAGNETIC Field Sensor Method *IEEE Trans. on Magnetics*, vol 48(11), p 4554-4557

[5] Piergentili F, Candini G P, and Zannoni M 2011 Design, Manufacturing and Test of a Real-Time Three-Axis Magnetic Field Simulator *IEEE Trans. on Aerospace and Elect. Sys.*, vol 47(2), p 1369-1379.

[6] Daniel S B, FRANCISCO G JR, MARCELO C T, Leonimer F M 2018 Three-axial Helmholtz coil design and validation for aerospace application *IEEE Trans. on Aerospace and Elect. Sys.*, vol 54(1), p 392-403.
[7] https://demonstrations.wolfram.com/SquareHelmholtzCoils/.
[8] Honeywell AN-201, "Set/Reset Pulse Circuits for Magnetic Sensors", https://neurophysics.ucsd.edu/Manuals/Honeywell/AN-201.pdf.